

## Supplemental Data

### Luminex Specificity Assay for Class II MHC Products.

Recognition of human Class II MHC products by VHH4 was assessed for binding to HLA class II using the OneLambda class II single antigen kit. HLA-DRB and HLA-DQB antigen-coated Luminex<sup>®</sup> beads (1) were incubated with 10 µg/ml of Alexafluor532-conjugated VHH4 in 96 well plates, in conjunction with the manufacturer's reagents. The mixture was incubated for 30 min in the dark, at room temperature, on a rotating platform. The wells were then washed three times to remove unbound excess VHH4. After incubation, the plate was ready for data acquisition using Luminex<sup>®</sup>200<sup>™</sup>. Data acquired by the Luminex<sup>®</sup> software were imported into HLA Fusion<sup>™</sup> analysis software and results were analyzed as per manufacturer's recommendations.

### Generation and Housing of the BLT Model

BLT mice were prepared as described (2). Briefly, NSG mice, 6–8 weeks old, were sublethally (2Gy) irradiated, anesthetized, and 1 mm fragments of human fetal thymus and liver (Advanced Bioscience Resources) were implanted under the kidney capsule. CD34+ cells were isolated from fetal liver by means of anti-CD34 microbeads (Miltenyi).  $1 \times 10^5$  cells were injected intravenously within 6 hours after surgery. All surgery was performed under anesthesia and every effort was made to alleviate associated suffering. All mice were housed in micro-isolator cages in a specific pathogen-free facility, in accordance with Institutional Animal Care and Research Committee-approved protocols at Massachusetts General Hospital. All the mice that entered experiments had reached the standards that were highest in the literature. More than 25% of all cells had to be lymphocytes. From that number 50% had to be human (huCD45+) and from that number 40% had to be huCD3 positive (the majority of the mice in the experiment were higher than the standard). Absolute number of cells were counted using beads and only mice with more than 200 huCD4 cells per 100 µL of blood were selected. Mice that were below the standard cut-line did not enter the experiment. GvHD was scored by the following criteria; stage 0: unaffected, stage 1: blepharitis/conjunctivitis, stage 2: facial and/or surgical site alopecia, stage 3: Full body alopecia. The Massachusetts General Hospital Institutional Animal Care and Research Committee approved this study.

### Enzymatic Modification of Single Domain Antibodies using Sortase.

The penta-mutant sortase A, with an improved  $k_{cat}$ , was used (3). Reaction mixtures (1 mL) contained Tris-HCl (50 mM, pH 7.5), CaCl<sub>2</sub> (10 mM), NaCl (150 mM), triglycine-containing probe (500 µM), LPETG-containing probe (100 µM), and sortase (5 µM). After incubation at

4 °C with agitation for 1 h, reaction products were analyzed by LC-MS, with yields generally >90%. When the yield was below 90%, the reaction was allowed to proceed for an additional hour, with addition of sortase to 10  $\mu$ M and triglycine-containing probe to 750  $\mu$ M. Ni-NTA beads were added to the reaction mixture with agitation for 5 min at 25 °C, followed by centrifugation to remove sortase and any remaining unreacted His-tagged substrate. The final product -either the fluorophore-labeled VHH, or NOTA-labeled VHH, was purified by size exclusion chromatography in PBS or Tris·HCl (50 mM, pH 7.5). The labeled VHH was stored at -20 °C with 5% glycerol and was stable for at least six months.

### **Flow Cytometry**

All antibodies for flow cytometry were obtained from BD Biosciences: CD3, CD8, CD19, HLA-DR and CD45. Cells were incubated with antibodies at appropriate dilutions for 30 minutes at room temperature. Analyses were performed on a LSRFortessa flow cytometer (BD Biosciences) and analyzed with BD CellQuest Pro 6.0 software (BD Biosciences) and FlowJo version 10 software (TreeStar, Ashland, OR).

### **Multi-photon Imaging**

Two-photon imaging was performed as described before (4).

### **Synthesis of (Gly)<sub>3</sub>-Cys-NOTA.**

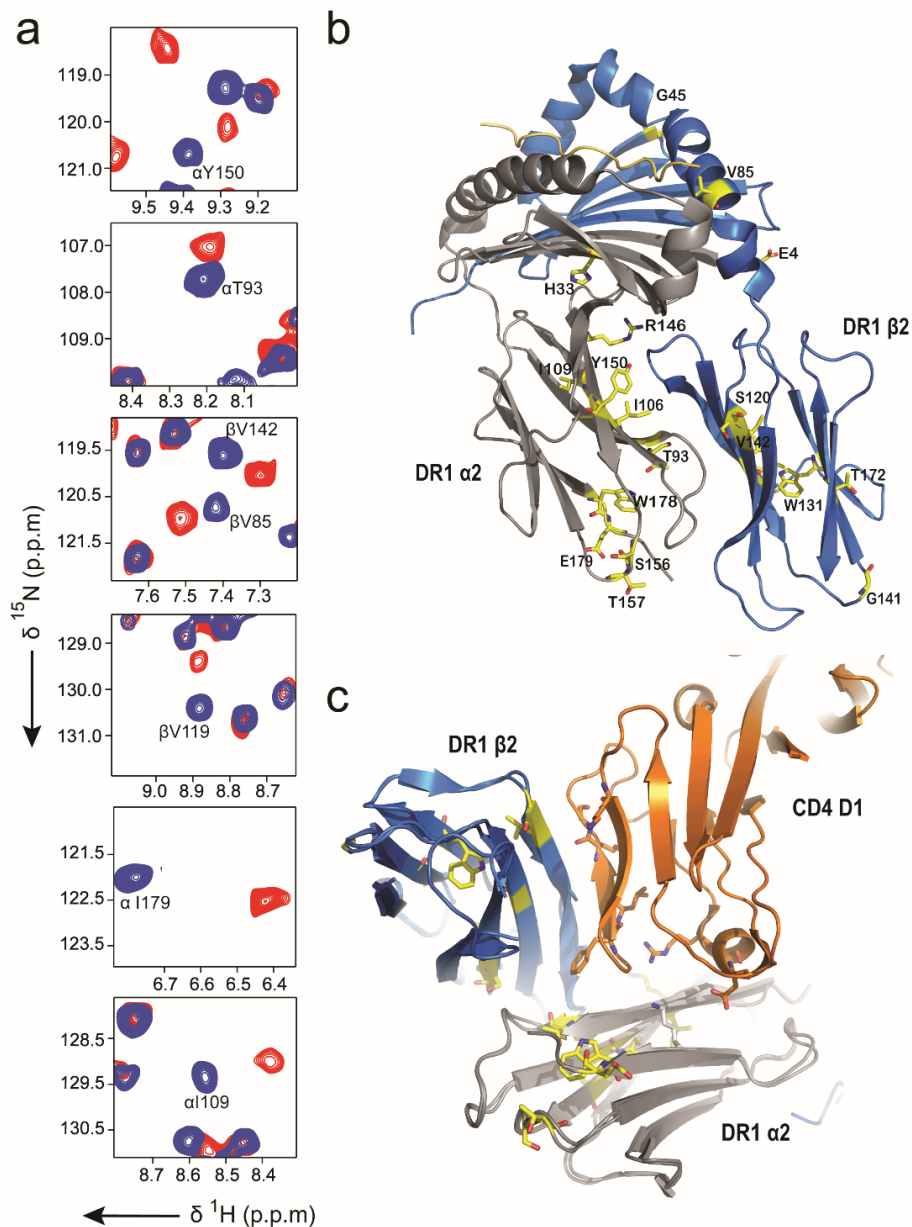
(Gly)<sub>3</sub>-Cys-NOTA was synthesized as described before (4).

### **Synthesis of <sup>64</sup>Cu-VHHs.**

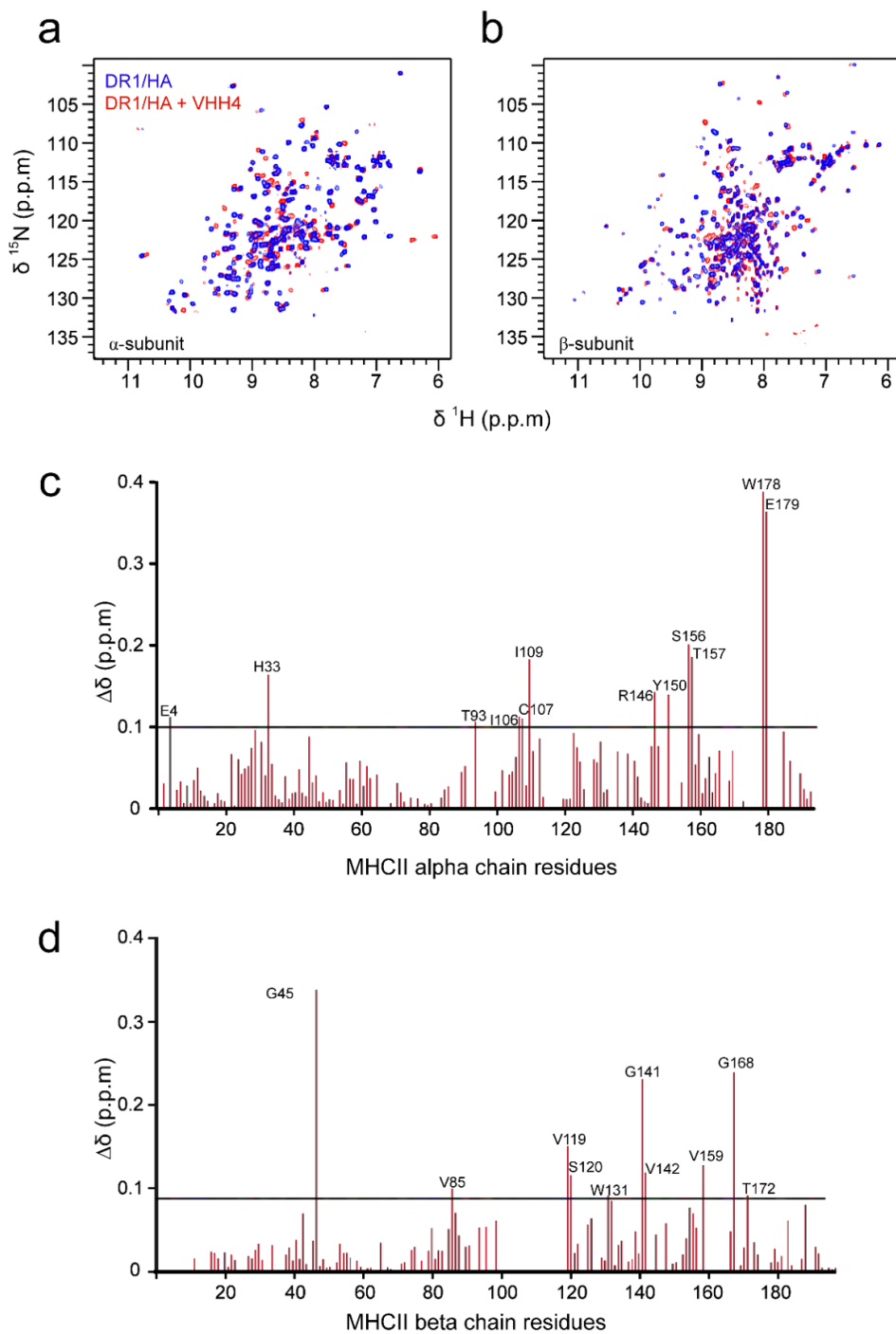
<sup>64</sup>Cu-VHH has been synthesized and characterized as reported (4).

### **PET-CT Imaging.**

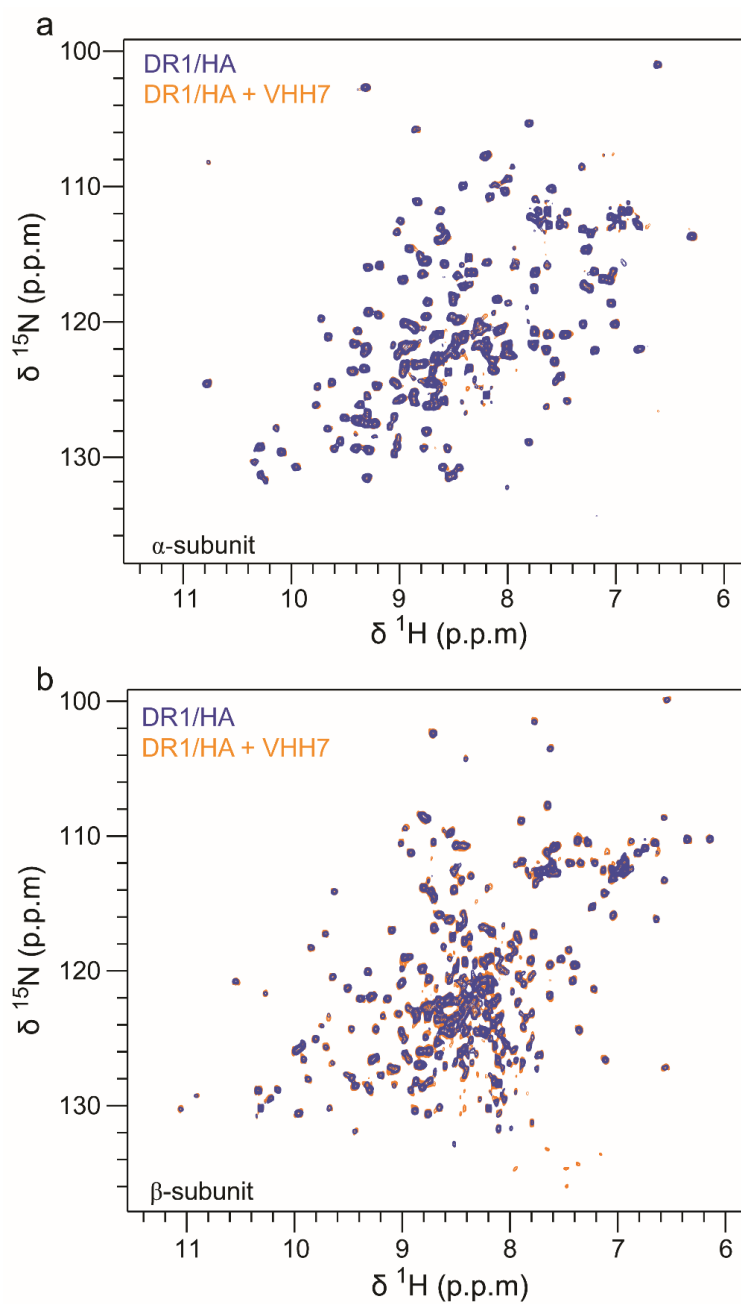
PET-CT procedures have been described in detail (4). For all imaging experiments, mice were anaesthetized using 2.0% isoflurane in O<sub>2</sub> at a flow rate of ~1 L/min. Mice were imaged with PET-CT using a G8 PET-CT small-animal scanner (Perkin Elmer). Peak sensitivity of the G8 PET-CT accounts for > 14% of positron emission, with a mean resolution of 1.4 mm. Each PET acquisition took 10 min followed by a 1.5 min CT scan. The images were reconstructed using the manufacturer's automatic image reconstruction software. Data were further analyzed and quantified using VivaQuant software. Two-dimensional and 3D visualizations were produced using the DICOM viewer OsiriX (OsiriX Foundation).



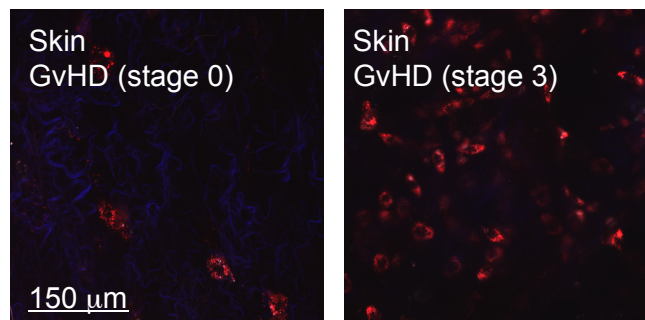
**Supplemental Figure 1.** (A) Magnification of selected regions from  $^1\text{H}$ - $^{15}\text{N}$ -HSQC spectra of free HLA-DR1/HA (blue) overlaid with a spectrum of a 1:1 complex of HLA-DR1/HA/VHH4 (red) (B) Residues displaying significant chemical shift differences upon interaction with VHH4 are shown as yellow sticks in the HLA-DR1/HA structure (PDB:1DLH) (5). (C) Superposition of HLA-DR1/HA (PDB: 1DLH) (5) and HLA-DR1/HA in complex with CD4 (PDB: 3S4S) (6). Close up view on the interface formed by CD4 D1 domain (orange) and DR1  $\alpha 2$  (grey) and  $\beta 2$  (blue) domains. HLA-DR1 residues displaying significant chemical shift differences upon interaction with VHH4 are represented as yellow sticks. CD4 D1 residues involved in the interaction with HLA-DR1 are represented in orange (6).



**Supplemental Figure 2:**  $^1\text{H}$ - $^{15}\text{N}$ -HSQC spectra show binding of VHH4 to HLA-DR1/HA. (A) Overlay of  $^1\text{H}$ - $^{15}\text{N}$ -HSQC spectra of  $^{15}\text{N}\alpha$ -labeled free HLA-DR1/HA (blue) and of a 1:1 complex of  $^{15}\text{N}\alpha$ -labeled HLA-DR1/HA and VHH4 (red). (B) Same representation as in A but for  $^{15}\text{N}\beta$ -labeled HLA-DR1. (C) Plot of chemical shift differences observed in HLA-DR1  $\alpha$ -chain upon the addition of equimolar amounts of VHH4. (D) Same representation as C but for  $\beta$ -chain. In C and D, a black horizontal line indicates the significance cut off. Bars corresponding to residues displaying significant chemical shift differences are labeled.



**Supplemental Figure 3:** Overlay of  $^1\text{H}$ - $^{15}\text{N}$ -HSQC NMR spectra of  $^{15}\text{N}\alpha$ -labeled HLA-DR1 (A) and  $^{15}\text{N}\beta$ -labeled HLA-DR1 (B) alone (blue) and upon addition of equimolar amounts of VHH7 (orange).



**Supplemental Figure 4.** Two-photon analysis of VHH4 signal in skin after signal saturation. Mice with and without clinical symptoms of GvHD were injected with large amounts of VHH4-TexasRed (150  $\mu$ g). Mice were sacrificed 2 h post injection to collect skin for two-photon microscopy. Left panel: No GvHD (stage 0), Right panel: GvHD stage 3.

## REFERENCES

1. Tait BD, Hudson F, Cantwell L, et al. Review article: Luminex technology for HLA antibody detection in organ transplantation. *Nephrology (Carlton, Vic)*. 2009;14:247-254.
2. Brainard DM, Seung E, Frahm N, et al. Induction of robust cellular and humoral virus-specific adaptive immune responses in human immunodeficiency virus-infected humanized BLT mice. *Journal of Virology*. 2009;83:7305-7321.
3. Chen I, Dorr BM, Liu DR. A general strategy for the evolution of bond-forming enzymes using yeast display. *Proceedings of the National Academy of Sciences of the United States of America*. 2011;108:11399-11404.
4. Rashidian M, Keliher EJ, Bilate AM, et al. Noninvasive imaging of immune responses. *Proceedings of the National Academy of Sciences of the United States of America*. 2015;112:6146-6151.
5. Stern LJ, Brown JH, Jardetzky TS, et al. Crystal structure of the human class II MHC protein HLA-DR1 complexed with an influenza virus peptide. *Nature*. 1994;368:215-221.
6. Wang XX, Li Y, Yin Y, et al. Affinity maturation of human CD4 by yeast surface display and crystal structure of a CD4-HLA-DR1 complex. *Proceedings of the National Academy of Sciences of the United States of America*. 2011;108:15960-15965.